JOURNAL OF Materials CHEMISTRY

New conductive molecular composites: aniline derivatives as guest molecules encapsulated and polymerized within the channels of the host 3D-coordination polymers $[(Me_3E)_3Fe(CN)_6]_\infty$ where E = Sn or Pb

Amany M. A. Ibrahim

Department of Chemistry, Faculty of Science, Ain Shams University, Cairo, Egypt

New conductive molecular composites have been prepared by chemical oxidation of polyanilines within the expandable wide channels of the 3D-coordination polymers $[(Me_3E)_3Fe(CN)_6]_\infty$ where E = Sn or Pb, in the presence and absence of HCl. The UV and visible absorption spectra of the protonated and deprotonated molecular composites are compared with those of polyanilines, polyemeraldine and nigrosine. The protonated molecular composites exhibit conductivities higher than the deprotonated ones. Also, polymerization of some aniline derivatives within the channels of the 3D-polymers, in absence of HCl, leads to vast improvement in conductivity owing to self protonation of the polyemeraldine base. The dramatic shift in optical response of the molecular composite containing polyemeraldine base with change in pH could be used as an optical pH sensor over the pH range investigated.

Introduction

The interest in composite materials formed from conducting polymers and conventional polymers is sparked by a desire to couple the physical properties of conventional polymers with the conductivity exhibited by conducting polymers.[1–3] The attractive characteristic features of 3D-coordination polymers of the type $[(Me_3E)_3M(CN)_6]_\infty$ suggested the idea that aniline and its derivatives could be encapsulated into the expandable channels of these polymers to yield conductive molecular composites.[4] These coordination polymers can be synthesized by the reaction of organotin(IV) or organolead(IV) compounds with hexacyano–d-transition metal ions (Fe and Co) to form unprecedented modes of supramolecular architecture having three-dimensional polymeric networks.[5,6] These 3D-polymers have zeolite like structures involving $Me_3E(NC)_2$ units with trigonal bipyramidal configuration and remarkably wide parallel channels with cross-sections of *ca.* 10×10 Å, whose walls are internally coated by constituents of the lipophilic Me_3E groups.[6]

The choice of polyaniline and its derivatives is due to their many interesting properties. Such properties make polyanilines suitable for applications such as: materials for modified electrodes,[7–10] corrosion inhibitors for semiconductors in photoelectrochemical assemblies,[11] in microelectronics,[12,13] electrochromic materials,[14–17] in rechargeable lithium batteries,[18–21] in high-resolution light images[22] and recently in developing a conductive molecular 'wire' of near-molecular dimensions[23] where the polyaniline filaments are essentially 3 nm wide because they are formed inside the channels of an aluminosilicate crystal with 3 nm diameter pores.

Polyanilines represent a class of polymers built up from benzenoid (A) and quinonoid (B) repeat units. The combination of one (A) and one (B) unit comprises 'emeraldine' whereas four (B) moieties constitute 'nigrosine'; which is also referred to as 'nigraniline'. However, polyanilines exhibit a much greater complexity of properties and structure which are mainly due to the different preparation conditions.

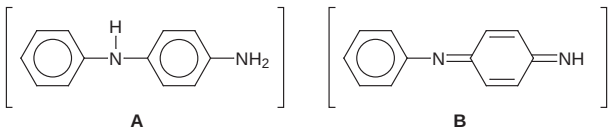

Polyanilines can be readily protonated and deprotonated,[24] and yet the number of electrons on the polymer chain remains constant. This has led to the proposal of a two-dimensional surface to adequately describe the state of the polymer.[25,26] However, there are still a great deal of unresolved details concerning the structure of the polymer chain, and the conformational and electronic changes.

Here, the electronic absorption spectra of polyaniline and its derivatives encapsulated within the channels of the 3D-polymers $[(Me_3E)_3M(CN)_6]_\infty$ (E = Sn or Pb) are studied and compared with those of benzene, aniline, nigrosine and polyemeraldine described quantitatively by CNDO/S_3 configuration-interaction (CI) calculations.[27,28]

Experimental

The host 3D-polymers were prepared by dissolving a 3:1 molar ratio of Me_3SnCl or Me_3PbCl and $K_3Fe(CN)_6$ in the minimum amount of water under a nitrogen atmosphere in the dark to yield $[(Me_3Sn)_3Fe(CN)_6]_\infty$ **I** and $[(Me_3Pb)_3Fe(CN)_6]_\infty$ **II**. The precipitates were filtered off, washed with water then CH_2Cl_2 and dried under vacuum at room temperature. The purity and identity of these 3D-polymers were checked as described elsewhere,[4,6] Table 1. Aniline derivatives were doubly distilled under reduced pressure while the solid starting materials were of highly pure grade purchased from Aldrich or Merck. A cold (5 °C) 1 M HCl solution, containing an excess of ammonium peroxodisulfate with respect to the desired reaction stoichiometry was added dropwise to a cold, stirred solution of aniline derivatives in 1 M HCl to yield black polyaniline **1′**, poly(*o*-toluidine) **2′**, poly(*m*-toluidine) **3′**, dark brown poly(*p*-toluidine) **4′**, black poly(*o*-anisidine) **5′**, poly(*p*-anisidine) **6′**, poly(2-chloroaniline) **7′**, poly(3-chloroaniline) **8′**, brown poly(4-chloroaniline) **9′**, and greenish brown poly(2,4,6-trimethylaniline) **10′**. The molecular composites were prepared by the addition of cold (< 5 °C) aniline derivatives to the cold freshly prepared 3D-polymer **I** or **II**, suspended in a minimum amount of water, in a molar ratio of 3:1. This mixture was ground well in the absence of direct light for at least 30 min and then left for about 10 days. The molecular composites, **1–10** obtained from polymer **I** and **11** and **12** obtained from polymer **II** were washed with ethanol and dried under vacuum. The compositions of these molecular

Table 1 Colour and elemental analysis of polymers **I**, **II** and their molecular composites

no.	compound	colour	elemental analysis found (calc.) (%)			
			C	H	N	Fe
I	$[(Me_3Sn)_3Fe(CN)_6]_\infty$	orange	25.61 (25.76)	3.87 (3.93)	11.94 (11.87)	7.94 (7.86)
II	$[(Me_3pb)_3Fe(CN)_6]_\infty$	yellowish orange	18.59 (18.26)	2.81 (3.02)	8.67 (8.34)	5.76 (5.68)
1	$[(aniline)_{1.5}+\mathbf{I}]_n$	black	34.19 (34.10)	4.48 (4.62)	12.46 (11.98)	6.62 (6.42)
2	$[(o\text{-toluidine})_{1.5}+\mathbf{I}]_n$	black	35.44 (35.30)	4.72 (4.92)	12.15 (12.00)	6.46 (6.18)
3	$[(m\text{-toluidine})_{1.5}+\mathbf{I}]_n$	black	35.44 (35.40)	4.72 (4.87)	12.15 (11.98)	6.46 (6.25)
4	$[(p\text{-toluidine})_{1.25}+\mathbf{I}]_n$	dark brown	34.06 (34.20)	4.57 (4.82)	12.13 (11.99)	6.66 (6.51)
5	$[(o\text{-anisidine})_{1.5}+\mathbf{I}]_n$	black	34.48 (34.31)	4.59 (4.84)	11.89 (11.21)	6.28 (6.30)
6	$[(p\text{-anisidine})_{1.5}+\mathbf{I}]_n$	black	34.48 (34.28)	4.59 (4.91)	11.89 (11.52)	6.28 (6.18)
7	$[(o\text{-chloraniline})+\mathbf{I}]_n$	black	30.35 (30.26)	4.00 (4.12)	11.80 (11.20)	6.72 (6.53)
8	$[(m\text{-chloraniline})+\mathbf{I}]_n$	black	30.35 (30.45)	4.00 (4.36)	11.80 (11.23)	6.72 (6.63)
9	$[(p\text{-chloraniline})_{0.9}+\mathbf{I}]_n$	brown	29.94 (29.90)	3.99 (4.34)	11.81 (11.42)	6.82 (6.72)
10	$[(2,4,6\text{-trimethylaniline})+\mathbf{I}]_n$	greenish brown	34.37 (34.25)	4.81 (4.67)	11.69 (11.29)	6.66 (6.63)
11	$[(aniline)_{1.5}+\mathbf{II}]_n$	black	28.98 (28.71)	3.80 (3.72)	10.56 (10.21)	20.83 (20.62)
12	$[(o\text{-anisidine})_{1.5}+\mathbf{II}]_n$	black	29.46 (29.31)	3.92 (4.12)	10.10 (9.72)	19.93 (19.72)

composites were investigated by elemental analysis, Table 1. The protonated molecular composites, **1H–10H**, **11H** and **12H**, were prepared by the same procedure in the presence of 1 M HCl solution. They have the same colours as the corresponding polyaniline derivatives.

The electronic absorption spectra were recorded on Shimadzu 240 W and Perkin-Elmer Model Lambda 3B double-beam UV-VIS spectrophotometers within the wavelength range 200–1000 nm as Nujol mull matrices. Conductivity measurements of pressed pellets of diameter 0.45–0.5 cm and thickness 0.08–0.1 cm were performed at 298 K using the four-probe technique and a super Megohmmeter Model RM 170 instrument (Avo Ltd., Dover, England).

Results and Discussion

The electronic absorption spectra of the new molecular composites **1–12**, as Nujol mull matrices reveal mainly five absorption bands at 232–775 nm, Fig. 1 and 2 and Table 2. These bands are due to the electronic transitions of polyanilines and the anionic host 3*D*-polymers; tris(trimethyltin) (or lead) hexacyanoferrate(II). Thus, it would be of interest to investigate, separately, the spectra of the host 3D-polymers and those of the polyanilines. The spectra of the 3D-coordination polymers **I** and **II** in Nujol mull display three absorption bands at 220, 300 and 430 nm for **I** and at 225, 310 and 420 nm for **II**, respectively. The low energy band at 430 nm corresponds to $\pi^*\leftarrow\pi$ transitions of the $Fe^{III}(CN)_6$ building blocks. This band shifts to 320 and 325 nm in the spectra of the isostructural polymers $[(Me_3E)_4Fe(CN)_6]_\infty$, where E = Sn or Pb, respectively, and corresponds to $\pi^*\leftarrow\pi$ transitions of the $Fe^{II}(CN)_6$ building blocks. Thus, these 3D-polymers are excellent materials for both accommodating the polyanilines within their wide channels as well as being essentially optically transparent in the visible region. On the other hand, the spectra of polyanilines **1′–10′** exhibit five absorption bands at 210–550 nm, Table 3. The first three bands at 210–230, 235–245 and 280–300 nm resemble those of aniline and its derivatives and correspond to $^1B\leftarrow{}^1A$, $^1L_a\leftarrow{}^1A$ and $^1L_b\leftarrow{}^1A$ transitions within the individual benzenoid systems in polyanilines.[28] They are due to the localized $\pi^*\leftarrow\pi$ transitions within the phenyl moieties in the polymers as is commonly found in pendant group polymers.[29] They show a slight blue shift relative to those of aniline and its derivatives. The broad band at 400–450 nm resembles the visible band of the *in situ* optical absorption spectra of a polyaniline film on a conducting Pt

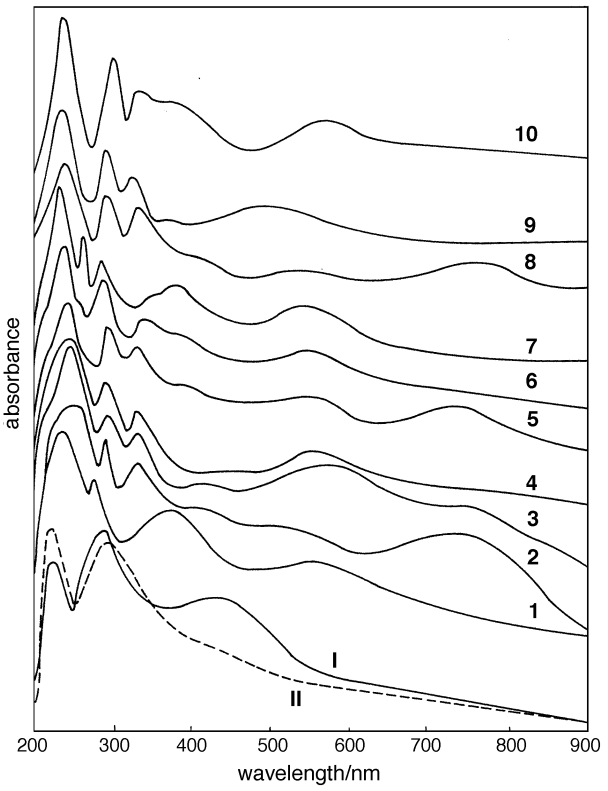

Fig. 1 The electronic absorption spectra of I, II and the molecular composites **1–10**

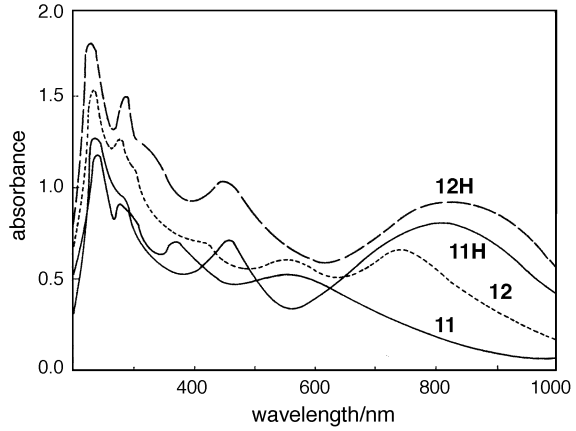

Fig. 2 The electronic absorption spectra of the molecular composites **11**, **12**, **11H** and **12H**

electrode as a function of the applied oxidation potential.[30] This band could be taken as indicative of polymerization and formation of polyemeraldine units rather than nigrosine units since it appears in the spectrum of polyemeraldine while it is not observed in the spectrum of nigrosine.[31] This is also supported by the presence of the band due to $\pi^*\leftarrow\pi$ transitions of nigrosine at 335–365 nm in the spectra of **6′**, **9′** and **10′**. Generally, $\pi^*\leftarrow\pi$ transitions are localized on benzenoid rings of the polyemeraldine units. The last band located at 540–560 nm arises from the charge transfer exciton from the benzenoid to quinoid segments ($\pi_Q\leftarrow\pi_B$) of the emeraldine base similar to bulk polyaniline.[32,33] The presence of this band presents also an indication of the polymerization of aniline and its derivatives where the λ_{max} for transitions of isolated chains should be much lower[34] as observed in the spectra of **6′** and **9′** (*ca.* $\lambda_{max}=450$ and 440 nm). According to the previous band assignment, the first two bands appearing around 240 and 280 nm in the spectra of the molecular composites **1–12** are due to $^1L_a\leftarrow{}^1A$ and $^1L_b\leftarrow{}^1A$ transitions within the individual benzenoid systems in polyanilines. The band at 320–340 nm is attributed to $\pi^*\leftarrow\pi$ transitions of the $Fe^{II}(CN)_6$ building blocks. The spectrum of **1** shows this as a broad composite band at 380 nm due to $\pi^*\leftarrow\pi$ transitions of both the $Fe^{II}(CN)_6$ building blocks and polyemeraldine. The presence of the band at 320–340 nm and the disappearance of the band at 420 nm can be considered as good evidence for the occurrence of a redox reaction between the host polymers and the aniline derivatives acting as guest molecules. The last band at *ca.* 550 nm corresponds to a molecular exciton bound to locally distorted segments of the oligomer backbone. The presence of this band is a further indication of the redox reaction and polymerization of polyanilines within the channels of the host polymers.

In addition to the above bands, the spectra of the molecular composites **2**, **3**, **5**, **8** and **12** exhibit a broad band at 730–775 nm. This band does not appear in the spectra of the corresponding polyanilines or those of the other molecular composites. To throw light on this band, the spectra of the molecular composites prepared in the presence of 1 M HCl were measured in Nujol mull matrices, Table 4 and Fig. 2. On protonation, the bands around 410 nm and 730–775 nm in the spectra of **2**, **3**, **5**, **8** and **12** exhibit high intensity and are red shifted. On the other hand, the spectra of the other protonated molecular composites show two absorption bands at 440–455 nm and 770–820 nm while the band around 550 nm disappears and the high energy bands ($\lambda_{max}<340$ nm) remain at more or less the same positions, Table 4.

These changes in absorption spectra upon protonation, are in accordance with the disappearance of the localised quinoid structure and the formation of a polaron lattice or bipolaron according to the following structures.

Table 2 The electronic absorption spectra of the molecular composites **1–12**

compound	$^1L_a\leftarrow{}^1A$	$^1L_b\leftarrow{}^1A$	$\pi^*\leftarrow\pi$ $Fe^{II}(CN)_6$	$\pi^*\leftarrow\pi$ polyemeraldine	CT-exciton $\pi_Q\leftarrow\pi_B$	bipolaron transitions
1	240	280	385	—	555	—
2	250	285	325	410	560	740
3	250	285	330	415	555	770
4	232	283	320	380	550w[a]	—
5	240	283	320	420	538	730
6	240	280	325	390	540	—
7	240	280	320	380	565	
8	242	285	330	410	520	775
9	245	285	335	390	480	—
10	245	285	340	410	580	—
11	240	285	310	380	570	—
12	240	280	305	420	560	750

[a]w = Weak.

Table 3 Electronic absorption spectra of polyanilines **1′–10′**

compound	$^1B\leftarrow{}^1A$	$^1L_a\leftarrow{}^1A$	$^1L_b\leftarrow{}^1A$	$\pi^*\leftarrow\pi$ polyemeraldine	CT-exciton $\pi_Q\leftarrow\pi_B$
1′	230	245	280	400	550
2′	220	235	300	—	550
3′	215	235	300	410	550
4′	220	241	300	415	540w[a]
5′	215	240	300	400	550
6′	210	240	300	360[b]	450
7′	215	240	280	415	550
8′	215	240	300	415	560
9′	215	236	280	335–365[b]	440
10′	218	245	300	340[b]	550w[a]

[a]w = Weak. [b]Nigrosine.

Table 4 The electronic absorption spectra of the protonated molecular composites **1H**–**12H**

compound	$\pi^*\leftarrow\pi$ polyemeraldine base	bipolaron transitions	compound	$\pi^*\leftarrow\pi$ polyemeraldine base	bipolaron transitions
1H	450	790	**7H**	440	770
2H	450	805	**8H**	450	810
3H	455	820	**9H**	440	760
4H	440	790	**10H**	445	770
5H	450	800	**11H**	450	795
6H	455	780	**12H**	445	800

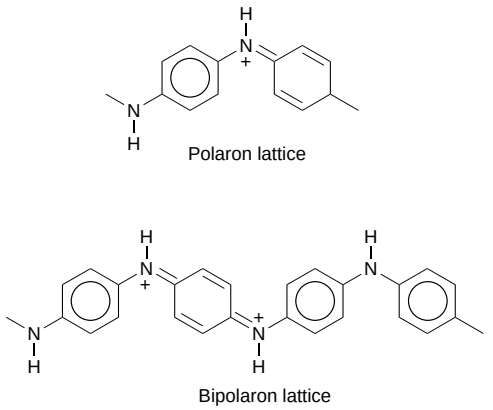

The presence of these polaron or bipolaron states would produce two levels in the gap with three allowed directed optical transitions for the polaron and two for the bipolaron.[32] Since the spectra comprise only two bands in the visible region, the bipolaron is the most favourable structure which may be formed upon protonation.

The spectra of the deprotonated molecular composites **2**, **3**, **5**, **8** and **12** show both bands due to an exciton (550 nm) and bipolaron lattice (730–775 nm). This is due to the fact that the monomers of the aniline derivatives are oxidatively polymerized within the channels of the host polymers, which are reduced to the isostructural anionic homologue $[(Me_3E)_3Fe^{II}(CN)_6^-]_\infty$, producing protons. These protons are captured by the negatively charged channels of the host polymer and can link some of the unprotonated imine nitrogens of the emeraldine base forming the partially protonated emeraldine. This implies the presence of a dynamic equilibrium proton transfer between the partially protonated emeraldine and the negatively charged channels of the polymer, Scheme 1.

The dramatic changes in the absorption spectra of the unprotonated and protonated molecular composites indicate that they can be used as optical pH sensors over a wide pH range. The Nujol mull matrix of the molecular composite **1**, containing the emeraldine base form, was soaked in solutions of different pH values up to pH 7 (the host polymer decomposes in alkaline media). It was removed after 5 min, dried and then recorded, Fig. 3. Both bands at 385 and 555 nm undergo gradual shift to longer wavelengths (*ca.* 450 and 790 nm) as the pH is decreased. The plot of the maximum absorption wavelengths as a function of pH gives a straight line within the pH range 1.1–5.1 while above this pH range a negative deviation was observed, Fig. 4.

Conductivity of the molecular composites

The molecular composites **1–8**, **11** and **12** behave as good semiconductors having conductivities in the range 6.3×10^{-2}–0.82×10^{-4} S cm^{-1} while **9** and **10** behave as weak semiconductors ($\sigma_{298}=3.2\times10^{-6}$ and 5.0×10^{-7} S cm^{-1}, respectively), Table 5. The conductivity increases by three orders of magnitude upon protonation of the molecular composites ($\sigma_{298}=5.3\times10^{-4}$–0.69 S cm^{-1}). The semiconducting character of these molecular composites was supported by studying the variation of DC-electrical conductivity as a function of temperature for the molecular composites, Fig. 5. In all cases, there are positive temperature coefficients of electrical conductivity indicating semiconducting behaviour. The activation energies of the protonated molecular composites [ΔE *ca.* 0.21 (**1H**), 0.24 (**5H**) and 0.21, 0.18 eV (**11H**)] are lower than the corresponding values of the nonprotonated ones

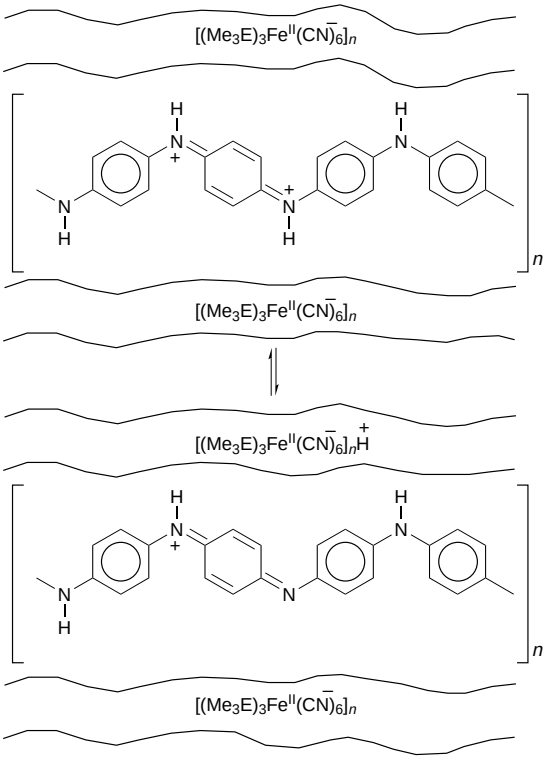

Scheme 1

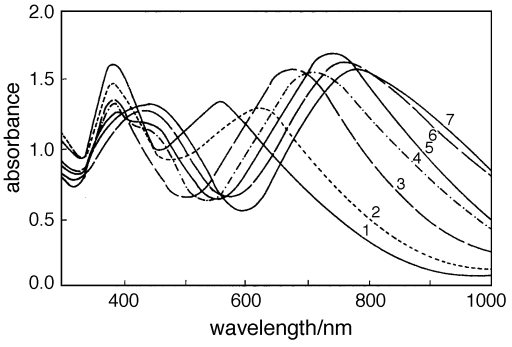

Fig. 3 The electronic absorption spectra of the molecular composite **1** doped in solutions of different pH values; 1 = 1.1, 2 = 2, 3 = 2.95, 4 = 4, 5 = 5.1, 6 = 6, 7 = 7

Table 5 Electrical conductivities at 298 K of the protonated and deprotonated molecular composites

compound	$\sigma_{298\ K}$/S cm^{-1}	compound	$\sigma_{298\ K}$/S cm^{-1}	compound	$\sigma_{298\ K}$/S cm^{-1}	compound	$\sigma_{298\ K}$/S cm^{-1}
1	2.2×10^{-4}	**7**	6.3×10^{-2}	**1H**	0.65	**7H**	0.19
2	3.6×10^{-2}	**8**	2.8×10^{-2}	**2H**	0.21	**8H**	0.15
3	5.8×10^{-2}	**9**	3.2×10^{-6}	**3H**	0.25	**9H**	2.8×10^{-3}
4	2.1×10^{-4}	**10**	5.0×10^{-7}	**4H**	0.02	**10H**	5.3×10^{-4}
5	2.1×10^{-2}	**11**	3.1×10^{-4}	**5H**	0.29	**11H**	0.69
6	8.2×10^{-5}	**12**	4.2×10^{-2}	**6H**	0.08	**12H**	0.30

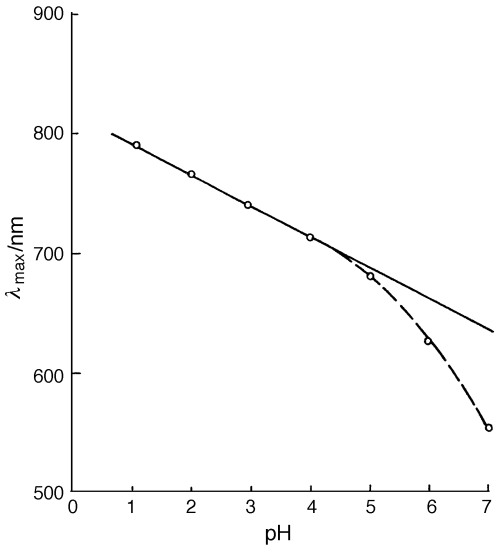

Fig. 4 The variation of the maximum absorption wavelength of the long wavelength band of the molecular composite **1** as a function of pH

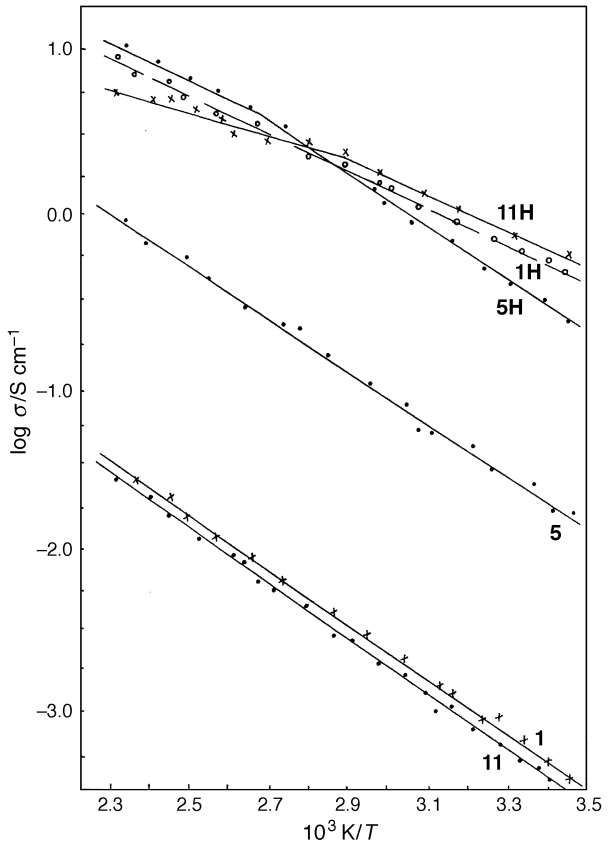

Fig. 5 log σ *vs.* 1000/T for the molecular composites **1**, **1H**, **5**, **5H**, **11** and **11H**

[ΔE *ca.* 0.33 (**1**), 0.31 (**5**) and 0.34 eV (**11**)] indicating that protonation facilitates the mobility of charge, and hence the protonated molecular composites would exhibit higher electrical conductivity than the corresponding non-protonated species. Derivatives with *ortho* and *meta* substituents exhibit higher conductivities than aniline and the other derivatives owing to the fact that incorporation of electron-donating substituents at the *ortho* or *meta* positions decreases the oxidation potential of the monomer[35,36] and hence the higher oxidation states are more facile to polymerize and consequently to be protonated by protons produced in the polymerization process. Also, the steric hindrance of the *meta* substituent or the presence of a substituent at the *ortho* position reduces side-coupling, producing more regular chains. In the case of aniline, molecular composites **1** and **11**, *para* coupling is not exclusive and radical cation coupling at the *ortho* position may lead to low yields of other products[37] causing a decrease in the conductivity. However, the protonated molecular composites **1H** and **11H** exhibit the highest conductivity. On the other hand, the molecular composites containing the *para*-substituted derivatives, **4**, **6** and **9** exhibit low conductivity due to the high possibility of radical cation coupling at the *ortho* position leading to a less planar conformation and consequently short conjugated chains.[37] For **10**, the presence of methyl groups makes the primary oxidation products rather less stable being more prone to polymerization and induces more deformation along the polymer backbone which results in a decrease of the degree of conjugation and hence a decrease in conductivity.

Conclusion

It has been demonstrated that novel conductive composites of 3D-coordination polymers and a variety of polyanilines can be prepared by chemical polymerization of polyanilines within the channels of the 3D-polymeric network. The improved conductivity of the deprotonated molecular composites is due to the presence of a dynamic equilibrium proton transfer causing partial protonation of emeraldine base and the formation of regular polyaniline chains, due to steric factors, into the channels of the polymeric network which prevent side-coupling. The protonated molecular composites exhibit a dramatic increase in conductivity due to the formation of bipolaron lattice. The optical response of the molecular composites towards acid–base conditions make their use as optical pH sensors possible. The characteristics of the composites can be varied by changing the aniline derivatives as well as the host matrix. Therefore, the molecular composites can be tailored to meet specific properties.

References

1 J. Yano, *J. Electrochem. Soc.*, 1991, **138**, 455.
2 X. Bi and Q. Pei, *Synth. Met.*, 1987, **22**, 145.
3 M. G. Kanatzidis, L. M. Tonge and T. J. Marks, *J. Am. Chem. Soc.*, 1987, **109**, 3797.
4 S. E. H. Etaiw and A. M. A. Ibrahim, *J. Organomet. Chem.*, 1993, **456**, 229.
5 P. Brandt, A. K. Brimah and R. D. Fischer, *Angew. Chem., Int. Ed. Engl.*, 1988, **27**, 1521.

6 U. Behrens, A. K. Brimah, T. M. Soliman, R. D. Fischer, D. C. Apperely, N. A. Davis and R. K. Harris, *Orgonometallics*, 1992, **11**, 1719.
7 A. F. Diaz and J. A. Logan, *J. Electroanal. Chem*., 1989, **111**, 111.
8 N. Oyama, Y. Chnuki, K. Chiba and T. Ohsaka, *Chem. Lett*., 1983, 1759.
9 K. Chiba, T. Ohsaka, Y. Ohnuk and N. Oyama, *J. Electroanal. Chem*., 1987, **219**, 117.
10 N. Oyama, T. Ohsaka and M. Nakanishi, *J. Macromol. Sci., Rev. Macromol. Chem., A*, 1987, **24**, 375.
11 R. Noufí, A. J. Nozik, T. White and L. F. Warren, *J. Electrochem. Soc*., 1982, **129**, 26.
12 E. P. Lofton, J. W. Thackeray and M. S. Wrighton, *J. Phys. Chem*., 1986, **90**, 6080.
13 S. Chao and M. S. Wrighton, *J. Am. Chem. Soc*., 1987, **109**, 6627.
14 T. Kobayashi, H. Yoneyama and H. Tamura, *J. Electroanal. Chem*., 1984, **161**, 419; **177**, 281, 293.
15 E. M. Geniès, M. Lapkowski, C. Santier and E. Vieil, *Synth. Met*., 1987, **18**, 631.
16 A. Watanabe, K. Mori, Y. Iwasaki, Y. Nakamura and S. Niizuma, *Macromolecules*, 1987, **20**, 1793.
17 A. Akhtar, H. A. Weakliem, R. M. Paiste and K. Gaughen, *Synth. Met*., 1988, **26**, 203.
18 T. Osaka, S. Ogano and K. Naoi, *J. Electrochem. Soc*., 1988, **135**, 539.
19 T. Osaka, S. Ogano, K. Naoi and N. Oyama, *J. Electrochem. Soc*., 1989, **136**, 306.
20 T. Osaka, T. Nakajime, K. Naoi and B. Owens, *J. Electrochem. Soc*., 1990, **137**, 2139.
21 E. M. Gènies, P. Hany and C. Santier, *J. Appl. Electrochem*., 1988, **18**, 751.
22 H. Yoneyama, N. Takahashi and S. Kuwabota, *J. Chem. Soc., Chem. Commun*., 1992, 716.
23 C. G. Wu and T. Bein, *Last Week's Sci*., 1994, **264**, 1757.
24 E. J. C. Chiang and A. G. MacDiarmid, *Synth. Met*., 1986, **13**, 193.
25 W. R. Salaneck, I. Lundstrom, W. S. Huang and A. G. MacDiarmid, *Synth. Met*., 1987, **21**, 121.
26 E. M. Gènies and E. Viet, *Synth. Met*., 1987, **20**, 97.
27 W. R. Salaneck, I. Lundstrom, A. G. MacDiarmid and W. S. Huang, *Synth. Met*., 1986, **13**, 294.
28 N. O. Lipari and C. B. Duke, *J. Chem. Phys*., 1975, **63**, 1768.
29 C. B. Duke, *Mol. Cryst. Liq. Cryst*., 1979, **50**, 63.
30 A. P. Monkman, D. Bloor, G. C. Stevens and J. C. H. Stevens, *J. Phys. D: Appl. Phys*., 1987, **20**, 1337.
31 C. B. Duke, E. M. Conwell and A. Poton, *Chem. Phys. Lett*., 1986, **131**, 82.
32 A. J. Epstein and A. G. MacDiarmid, in *Electronic Properties of Conjugated Polymers*, ed. H. Kuzmany, M. Mehring and S. Roth, Springer, Berlin, 1989.
33 A. P. Monkman and P. Adams, *Synth. Met*., 1991, **40**, 87.
34 S. Stafström and J. L. Bredas, *Synth. Met*., 1989, **29**, E219.
35 M. Leclerc, J. Guay and L. H. Dao, *J. Electroanal. Chem*., 1988, **251**, 21; *Macromolecules*, 1989, **22**, 649.
36 Y. Wei, W. W. Focke, G. E. Wnek, A. Ray and A. G. MacDiarmid, *J. Phys. Chem*., 1989, **93**, 495.
37 L. T. Yu, M. S. Borredon, M. Jozefowicz, G. Belorgey and R. Buvet, *J. Polym. Soc*., 1987, **10**, 2931.

Paper 7/08827B; *Received* 8*th December*, 1997